NATIONAL ADVISORY COMMITTEE FOR AERONAUTICS

TECHNICAL NOTE 2379

AN INVESTIGATION OF THE EFFECTS OF JET-OUTLET CUT-OFF ANGLE ON THRUST DIRECTION AND BODY PITCHING MOMENT

By James R. Blackaby

Ames Aeronautical Laboratory
Moffett Field, Calif.

Washington
June 1951

NATIONAL ADVISORY COMMITTEE FOR AERONAUTICS

TECHNICAL NOTE 2379

AN INVESTIGATION OF THE EFFECTS OF JET-OUTLET CUT-OFF ANGLE ON THRUST DIRECTION AND BODY PITCHING MOMENT

By James R. Blackaby

SUMMARY

A wind-tunnel investigation was made to determine the effects of jet-outlet cut-off angle on the directional and spreading characteristics of an unheated, subsonic air jet, and on the pitching moment of the body from which the jet issued. The outlet was incorporated in the tail of an axially symmetric body and was cut at angles of 0°, 30°, 60°, and 75° relative to a plane normal to the outlet axis.

Force measurements showed that the net effect of cutting the outlet as much as 75° from normal was only a slight change of the pitching moment of the body. This change was probably caused primarily by external loads on the outlets.

In addition to the force measurements, visual studies were made of the flow in the jet exhausting from the outlets into still air. The characteristics of the flow in the jet observed in these studies were compared with characteristics shown by velocity profiles measured across air jets in other investigations.

INTRODUCTION

It was reported in reference 1 that a jet outlet bevelled 25° (i.e., cut off at an angle of 25° measured from a plane normal to the axis of the nozzle) caused little deflection of an unheated, subsonic air jet issuing from a cylindrical nozzle. The conclusions were based on tests in still air.

In order to ascertain whether greater jet-outlet bevel angles or external air flow affect the direction of an unheated, subsonic air jet, the present investigation was conducted in one of the Ames 7- by 10-foot wind tunnels. The forces on a body of revolution with a jet exhausting from a nozzle at the tail into both still and moving air were measured. The nozzle shape was changed by the use of four nozzle extensions which provided one outlet in a plane normal to the nozzle center line and three outlets in planes rotated 30°, 60°, and 75° from the plane of the normal

outlet. In addition to the wind-tunnel force tests, visual studies were made of the jet exhausting into still air.

NOTATION

The following symbols and subscripts are used in this report:

$\bar{c}$ mean aerodynamic chord of assumed wing, 1 foot

C_m pitching-moment coefficient about an axis at 39.35 percent of the body length $\left(\frac{\text{pitching moment}}{S\bar{c}q_o}\right)$

H total pressure, pounds per square foot

M Mach number

p static pressure, pounds per square foot

q dynamic pressure $\left(\frac{1}{2}\rho V^2\right)$, pounds per square foot

S assumed wing area, 10 square feet

V velocity, feet per second

α angle of attack, degrees

ρ mass density of air, slugs per cubic foot

Subscripts

j jet-outlet conditions

max maximum value for given station

o free-stream conditions

MODEL AND EQUIPMENT

The model used in the tests was a streamline body of revolution with an outlet at the tail. The basic body was 76.25 inches long and had a

maximum diameter of 12 inches at 39.35 percent of the length (figs. 1 and 2). Ahead of the maximum diameter, the body was ellipsoidal with a semimajor axis of 30 inches. A circular-arc fairing with a radius of about 42 inches formed the transition between the forebody and the afterbody which was conical. The diameter of the jet-outlet in the tail of the body was 2.43 inches.

The nozzle was machined to receive interchangeable extensions as shown in section A-A, figure 2. Tests were made with four nozzle extensions, one providing an outlet normal to the nozzle center line and the other three providing outlets bevelled 30°, 60°, and 75° measured from the plane of the normal outlet. (See fig. 3.)

The body was mounted in the wind tunnel on a single, tubular strut which, in turn, was supported in two ball bearings on the floating frame of the wind-tunnel balance. (See fig. 2.) The center line of the strut, and therefore the axis of rotation of the body, passed through the maximum diameter of the body.

The only restraint to the rotation of the body and strut, besides friction in the bearings which was considered to be negilgible, was that caused by a calibrated strain gage mounted as shown in section B-B of figure 2. The strain gage measured only the torque, or moment, about the center of rotation of the body. The lower end of the tubular strut fitted into a mercury seal and the upper portion, between the tunnel floor and the body, was shielded by a streamlined fairing visible in figure 1. A compressor outside the test chamber supplied air for the jet.

A total-pressure tube and a thermocouple were installed in a plenum chamber within the model, and each of the nozzles had a static-pressure orifice on its inner surface 0.25 inch ahead of the most forward point of the outlet. (See fig. 2.) These total- and static-pressure tubes were connected to a Machmeter, of the type described in reference 2, from which the Mach number at the outlet was read directly. The Mach number indicated by the Machmeter was within 0.01 of the Mach number determined from the pressure ratio across the nozzle.

TESTS AND TEST PROCEDURE

The body with each of the outlets was tested at angles of attack from -8° to +8° with jet-velocity ratios (V_j/V_o) of 0, 2.0, 3.0, and 4.0. The outlet diameter, 2.43 inches, was about one-seventh full scale compared with that for a representative jet engine having a static thrust of 4000 pounds. The jet-velocity ratios from 2.0 to 4.0 represent values encountered in full-scale aircraft operation at speeds from 700 to 300 miles per hour for altitudes up to 40,000 feet. The jet-velocity ratio for each jet Mach number and plenum-chamber temperature was varied by varying the tunnel speed.

In general, the tests were made with the highest practical tunnel speed and corresponding jet Mach number. The operating limitations were those imposed by the strength of the model and strain gage and by the capacity of the air compressor. The maximum tunnel speed with the body at zero angle of attack corresponded to a Mach number of about 0.30 and a Reynolds number of 2,100,000 per foot. The maximum jet velocity corresponded to a Mach number of 0.8 with a pressure ratio (p_j/H_j) of about 0.656. The dynamic pressures in the wind tunnel and the jet Mach numbers for all the tests with external air flow are presented in table I.

Visual studies of the flow from each of the outlets were made with the jet exhausting at Mach numbers of 0.6 and 0.8 into still air. Visualization of the flow along the plane of symmetry of the jet was accomplished by using jet-splitter plates mounted as shown in figure 4. The plates fitted closely outside the nozzles ahead of the outlets and extended inside the nozzles through the constant-area section to the low-speed region ahead of the nozzle contraction. A mixture of lampblack and kerosene, sprayed into the jets immediately after they emerged from the outlets, was deposited on the plates in the mixing regions of the jets. The patterns formed by the lampblack were photographed.

The sign convention used in expressing the pitching-moment coefficients for the body is shown in figure 5. To facilitate the tests, negative angles of attack were simulated by rotating the nozzle extensions 180°. This procedure was checked by testing the body with the 75°-bevelled outlet at an actual negative angle of attack. The resulting pitching moment was found to agree, within the experimental accuracy, with that for the body at the corresponding simulated negative angle of attack. For the calculation of pitching-moment coefficients from the strain-gage data, the model was assumed to have a wing with an area of 10 square feet and a mean aerodynamic chord of 1 foot in order that the coefficients would have the order of magnitude associated with a scale-model airplane having the test body as a fuselage. Thus,

$$C_m = \frac{\text{pitching moment}}{10\ q_o}$$

The model oscillated throughout the test because of minor flow fluctuations in the wind tunnel. The magnitude of the oscillations affected the strain-gage readings to the extent that the pitching-moment coefficients for the tunnel-on tests could be calculated with an accuracy of only ±0.001. No tunnel-wall corrections were applied.

RESULTS AND DISCUSSION

Jet Operating, Wind Tunnel Off

Figures 6 and 7 show the variation of the pitching moment and of the jet thrust with jet Mach number as determined from static tests. The pitching moment for the body with the normal, or 0°-bevelled, outlet was attributed to misalinement of the nozzle relative to the moment center. Therefore, these values of pitching moment were subtracted from the total static pitching moments for the other outlets to obtain the values shown by the dashed curves of static pitching moment attributed solely to asymmetrical jet action. The static pitching moment for the body with the 60°-bevelled outlet was estimated from cross plots of the data for the other three outlets. No measurements of nozzle coefficients were made in the present investigation.

As shown in figure 6, the pitching-moment increment attributed to asymmetrical jet action increased with increasing jet Mach number and with increasing outlet bevel angle, the maximum value being -1.26 pound-feet for the 75°- bevelled outlet with a jet Mach number of 0.8. The magnitude of the force necessary at the tail of the body to produce this moment was about that which would result from the action, on the asymmetrical outlet, of the static pressure differential which existed between the jet outlet and the still, external air, as determined utilizing the analysis in reference 3 for the mixing of a parallel stream with the adjacent air. The static pitching moment corresponded to a deflection of the jet-thrust direction at the outlet plane of only 0.3°. The value of the static pitching moment for the 75°-bevelled outlet with a jet Mach number of 0.8, if converted to a pitching-moment coefficient for a jet-velocity ratio of 4.0 (q_o = 58.8 pounds per square foot), would would be only -0.0021, which is only slightly larger than the experimental uncertainty of the tests.

Jet Off, Wind Tunnel Operating

The variations of the pitching-moment coefficients of the body with outlet bevel angle for the jet-off, tunnel-operating tests (V_j/V_o = 0) for angles of attack from -8° to +8° are shown in figure 8. The effect of tunnel airspeed on the pitching-moment coefficients was found to be small, so the curves represent averages applicable for all airspeeds in the test range. The curves indicate that the cross flow over the asymmetrical tail of the body as the outlet bevel angle increased to 60° caused a positive increment in the pitching-moment coefficient. However, for the extreme case of the 75°- bevelled outlet, the pitching-moment coefficients had decreased to values comparable with those for the 0°- and 30°- bevelled outlets.

Jet Operating, Wind Tunnel Operating

The curves of pitching-moment coefficient for the jet-on, tunnel-on tests are presented in figure 9 for jet-velocity ratios (V_j/V_o) of 2.0, 3.0, and 4.0. The increase of pitching-moment coefficient with increasing outlet bevel angle was probably due to a combination of the effects discussed in the two previous sections. However, the effect of asymmetrical jet action was shown to be very small, so the increments shown in figure 9 can be attributed almost entirely to the cross flow over the bevelled outlets. The reason the increments of pitching-moment coefficient with the jet operating (fig. 9) are less than those with the jet off (fig. 8), especially at positive angles of attack, is probably that the presence of the jet alleviated much of the effect of the cross flow over the outlets.

The curves in figure 10 show the effects of jet-velocity ratio and outlet bevel angle on the stability of the body more clearly and also emphasize that these effects were small. The variation of the pitching-moment coefficient with the angle of attack of the body with the 0°- and 75°-bevelled outlets is shown for each of the three jet-velocity ratios. In each case the body was unstable, but the effect of increasing the bevel angle was slightly stabilizing, especially at negative angles of attack. The effect of increasing the jet-velocity ratio was also slightly stabilizing, especially for the larger outlet bevel angles, and was probably the result of small changes in the external surface pressures near the jet outlet as the jet-velocity ratio was varied.

Flow Studies; Jet Operating, Wind Tunnel Off

Flow-study photographs of the jet issuing into still air from each of the outlets for jet Mach numbers of 0.6 and 0.8 are reproduced in figures 11 through 14. Because of the effects of boundary-layer growth along the plates and the interference of the plates with the jet, this flow visualization technique may not present an accurate measure of the characteristics of a free jet. However, the magnitude of these effects is probably small in the high-velocity central region of the jet where the flow patterns are sufficiently clear to permit comparison with jet characteristics determined from pressure surveys in references 1 and 4.

From measurements made on the photograph of the flow from the normal, or 0°-bevelled outlet, for a jet Mach number of 0.8 (fig. 15), the approximate boundaries of the jet (boundary A) and of the potential core (boundary B, enclosing the clear triangular area extending from the outlet, in which the velocity was equal to the velocity at the outlet) have been plotted nondimensionally in figure 16. Included in the figure are experimental points determined from velocity profiles measured in other investigations (references 1 and 4) designating jet and potential-core boundaries.

The potential-core boundary from the flow pictures (boundary B) agrees well with the experimental points, but the jet boundary (A) lies outside the boundaries determined from the velocity profiles, probably because of the boundary-layer and interference effects of the plates, mentioned previously, and because of the excess of the kerosene-lampblack mixture at the jet boundaries.

The asymmetry of flow in the mixing regions and around the potential core of the jet can be seen in the pictures for the bevelled outlets (figs. 11-14). One characteristic shown by these pictures is that the slope of the boundaries, or elements, of the potential core remained essentially constant for all the outlets, the effect of the bevel having been merely to translate elements of the core rearward. The apex of the core, therefore, was displaced from the center line of the nozzle as illustrated by the following sketch:

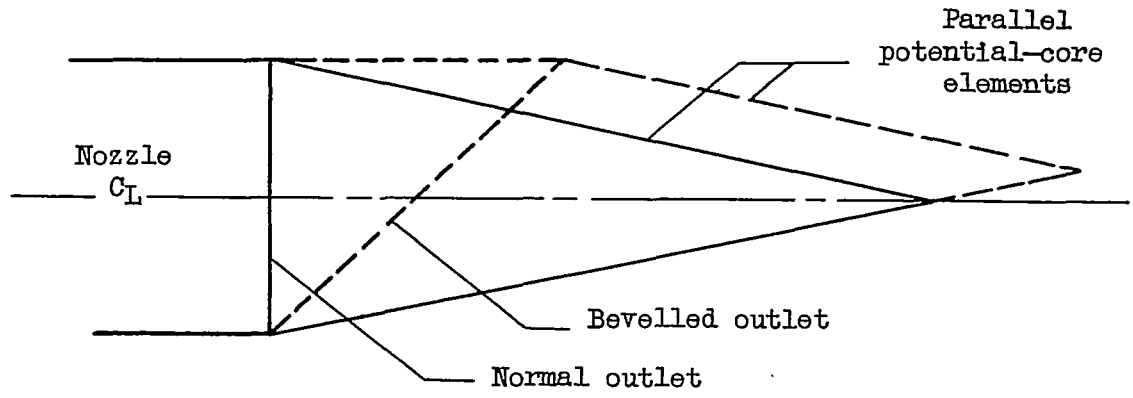

Insofar as the flow pictures afford a basis for a qualitative comparison of the characteristics of the flow from the various outlets (see figs. 11-14), two effects are worthy of mention. For the bevelled outlets, the potential-core boundary (B) varied in the manner just described, and the jet boundary (A) indicated an asymmetry in the spreading of the jet which became more pronounced as the outlet bevel angle was increased.

CONCLUDING REMARKS

Force tests made with a body of revolution with an unheated, subsonic jet of air exhausting from the tail showed that only small changes in pitching moment were caused by cutting off the outlet at angles of 30°, 60°, and 75°, measured from a plane normal to the outlet axis. The changes were the result of two opposing factors, a very small pitching-moment increment attributed to the asymmetrical action of the jet and a larger increment attributed to the asymmetry of the external forces on the bevelled outlets.

Visual studies of the flow in the jets exhausting into still air were compared with jet characteristics determined from velocity profiles measured in other investigations.

Ames Aeronautical Laboratory,
National Advisory Committee for Aeronautics,
Moffett Field, Calif., Mar. 9, 1951.

REFERENCES

1. Gillis, Clarence L., and Weil, Joseph: Some Notes on the Effects of Jet-Exit Design on Static Longitudinal Stability. NACA MR L6D30a, 1946.

2. Leipmann, Hans Wolfgang, and Ashkenas, Harry: Shock Wave Oscillations in Wind Tunnels. Jour. Aero. Sci., vol. 14, no. 5, May 1947, pp. 295-302.

3. Durand, William Frederick, Ed.: Aerodynamic Theory, vol. III, div. G, sec. 25. Pasadena California Institute of Technology, Jan. 1943.

4. Corrsin, Stanley: Investigation of Flow in an Axially Symmetrical Heated Jet of Air. NACA ACR 3L23, 1943.

TABLE I. – JET AND WIND-TUNNEL OPERATING CONDITIONS

V_j/V_o	α (deg)	M_j	q_o average (lb per sq ft)
2.0	±8	0.4	57.6
	±6	.5	90.0
	±4	.6	126.6
	±2	.6	126.6
	0	.6	126.6
3.0	±8	.7	77.6
	±6	.75	89.7
	±4	.8	101.3
	±2	.8	101.3
	0	.8	101.3
4.0	±8	.8	58.8
	±6	.8	58.8
	±4	.8	58.8
	±2	.8	58.8
	0	.8	58.8

(a) Front view.

(b) Rear view showing 60°–bevelled outlet.

Figure 1.– Test body installed in one of the Ames 7– by 10–foot wind tunnels.

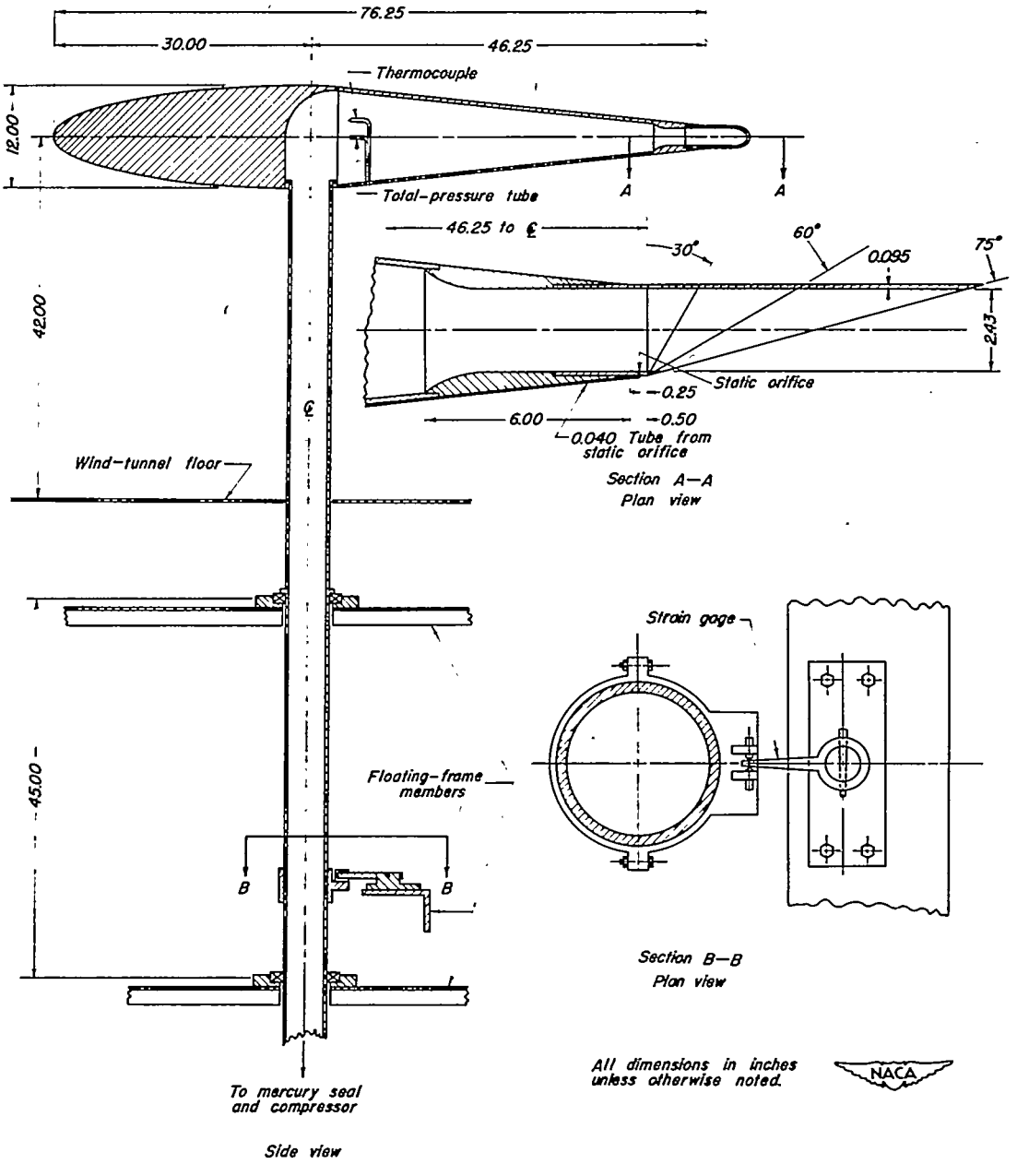

Figure 2.– Details of body-mounting method, nozzle installation, and strain-gage installation.

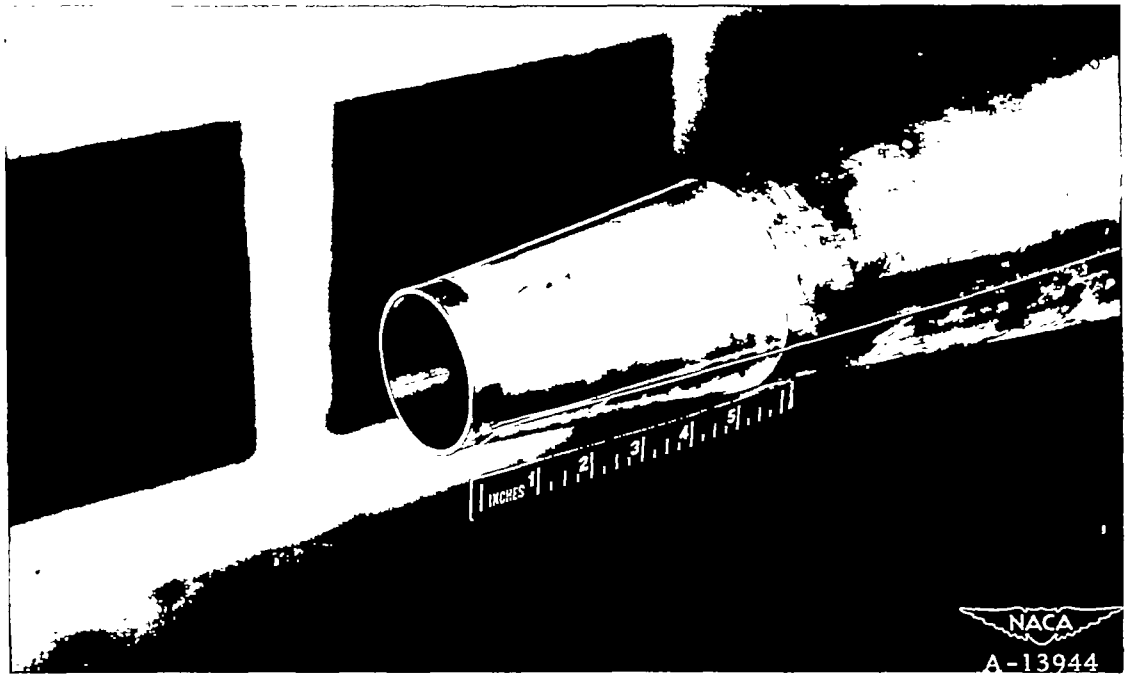

(a) 0°—bevelled outlet.

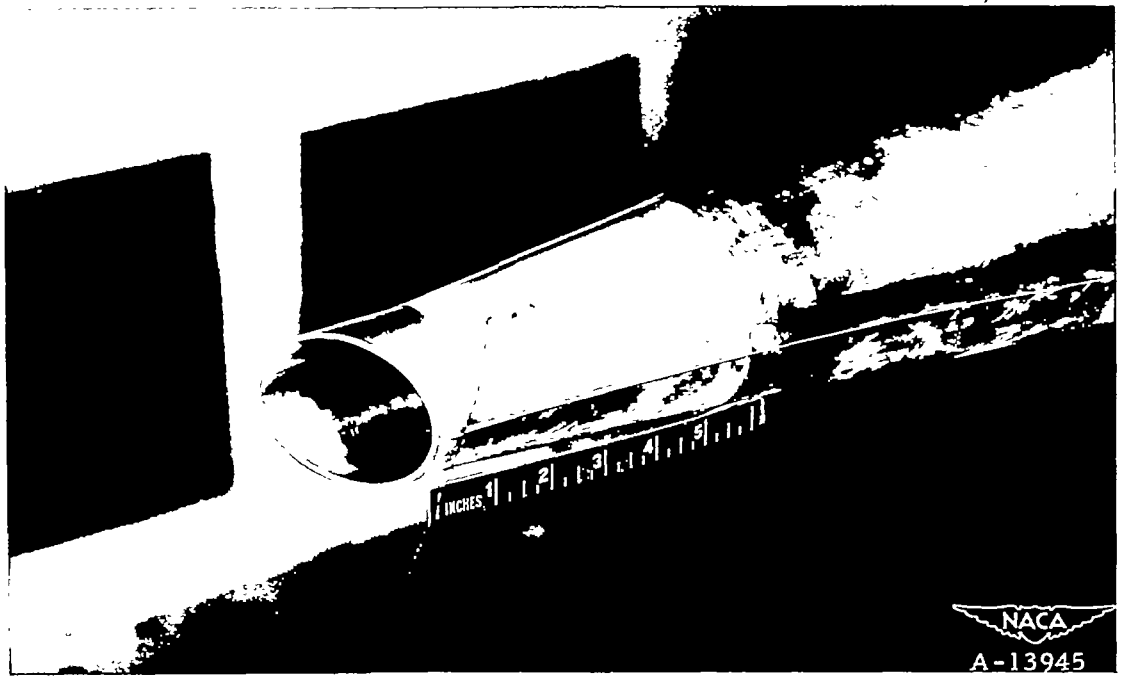

(b) 30°—bevelled outlet.

Figure 3.- Nozzles.

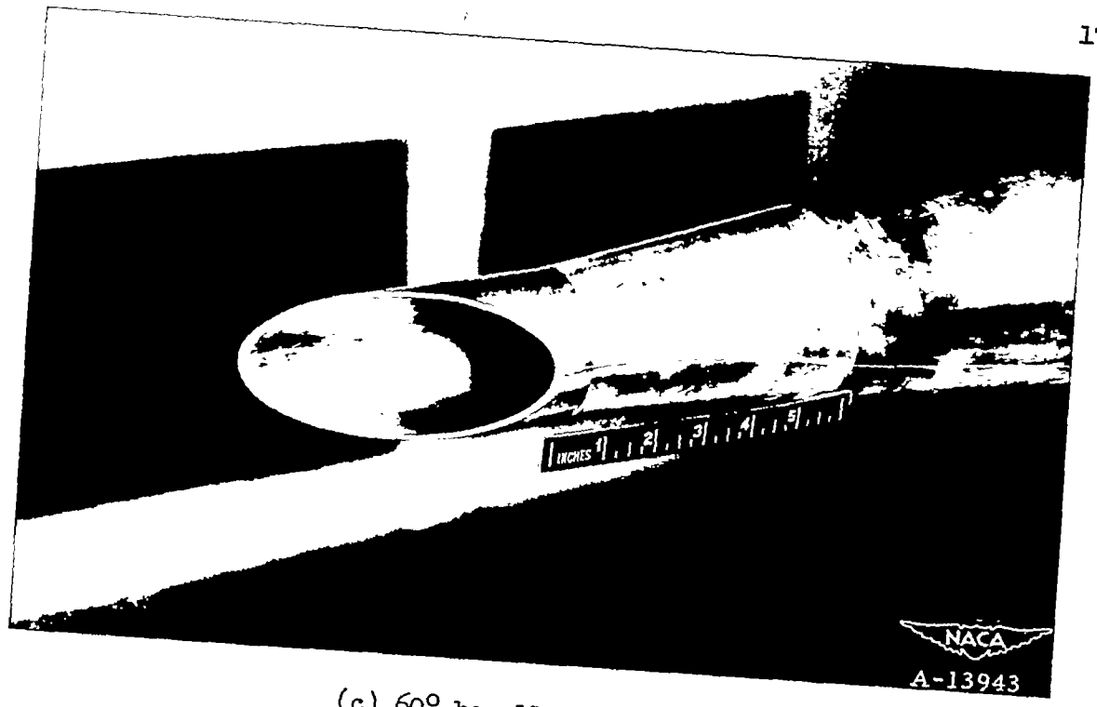

(c) 60°-bevelled outlet.

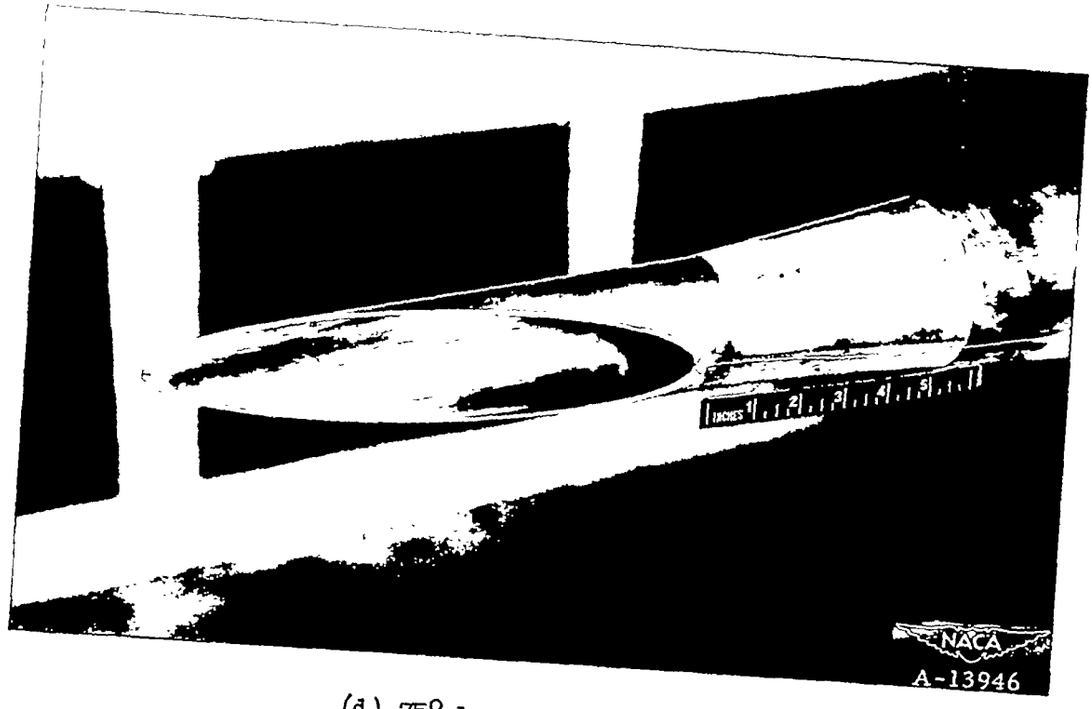

(d) 75°-bevelled outlet.

Figure 3.- Concluded.

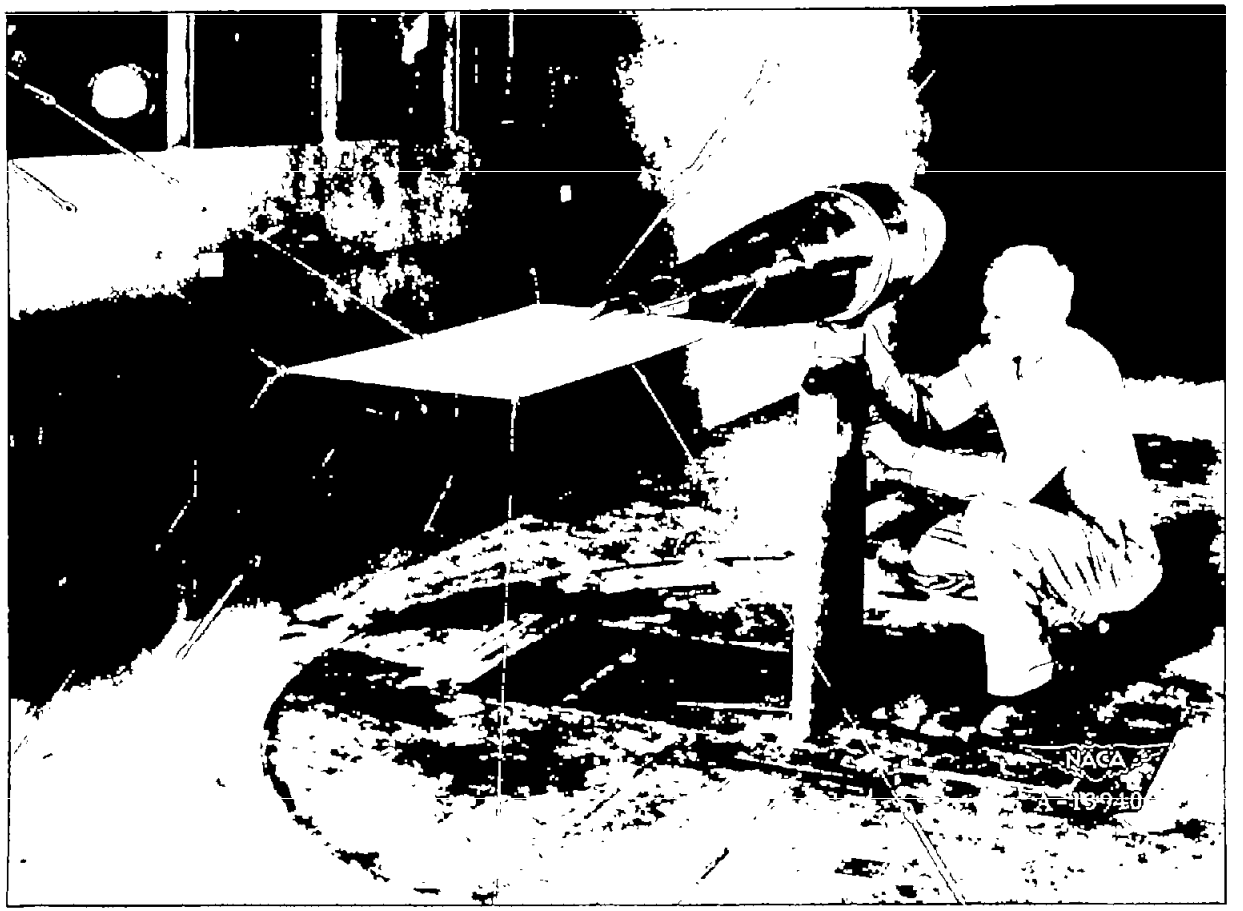

Figure 4.– Jet–splitter plate installed for flow visualization. 60°–bevelled outlet.

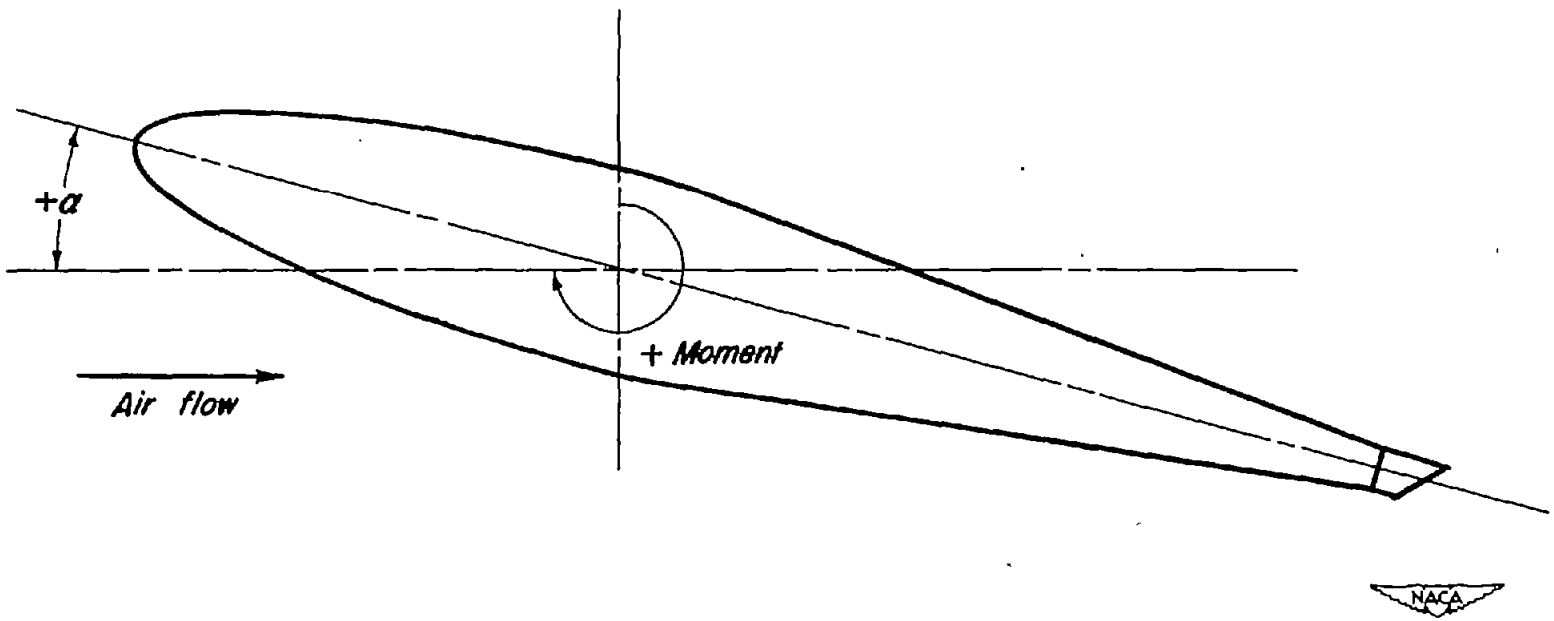

Figure 5.– Sign convention used in calculation of pitching moments.

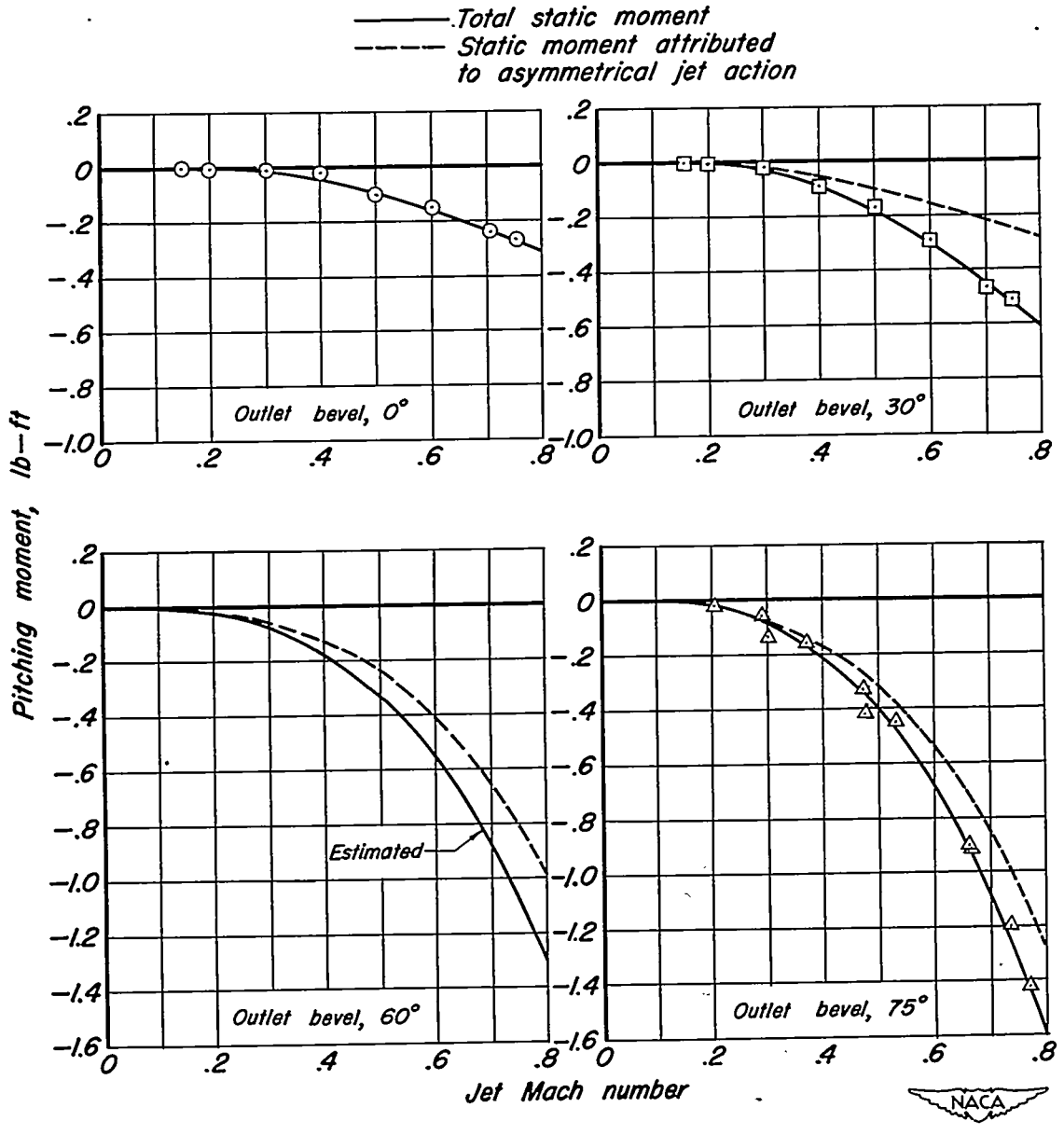

Figure 6.– Static pitching moment caused by jet issuing from bevelled outlet.

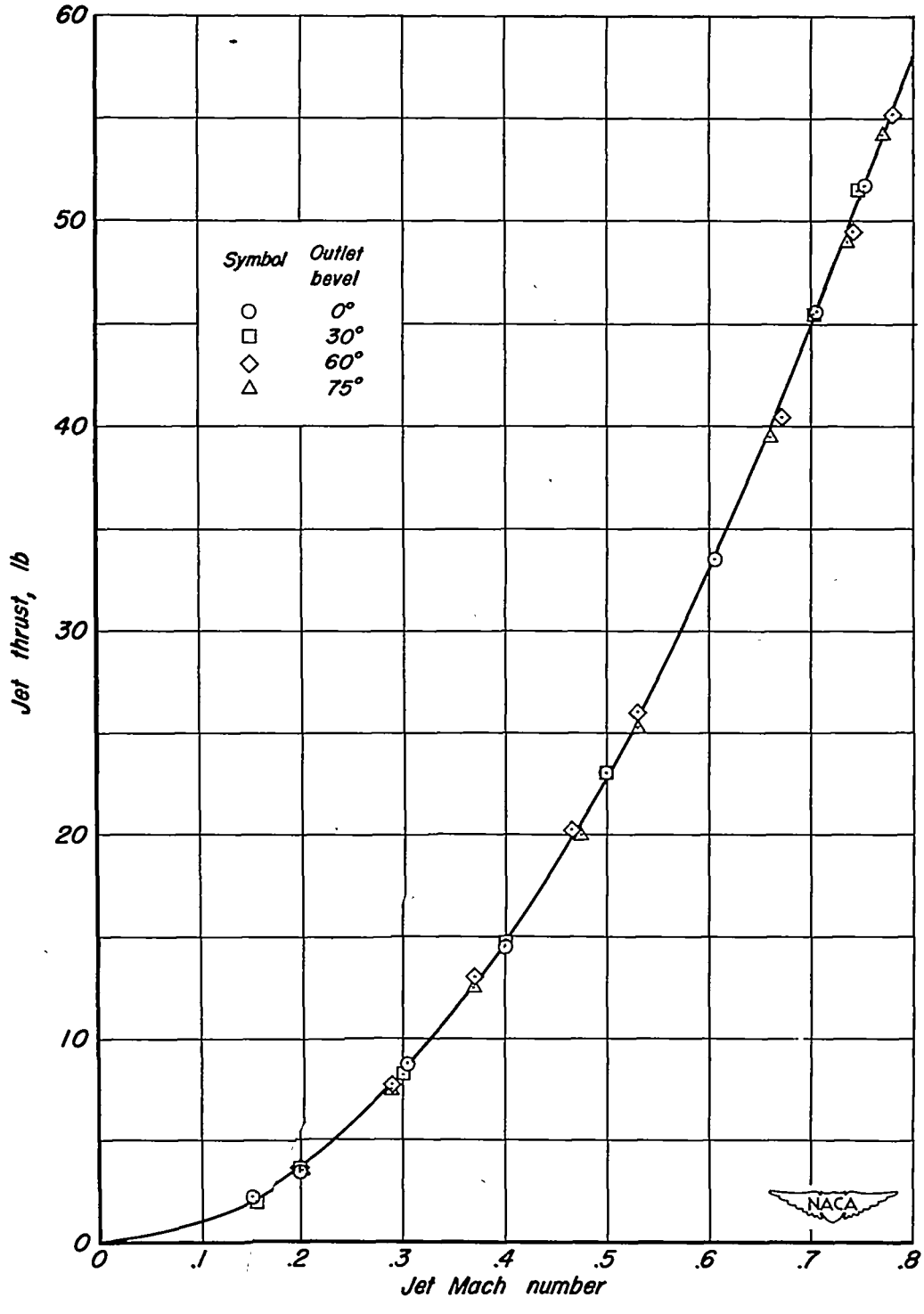

Figure 7.—Static thrust of jet issuing from bevelled outlets.

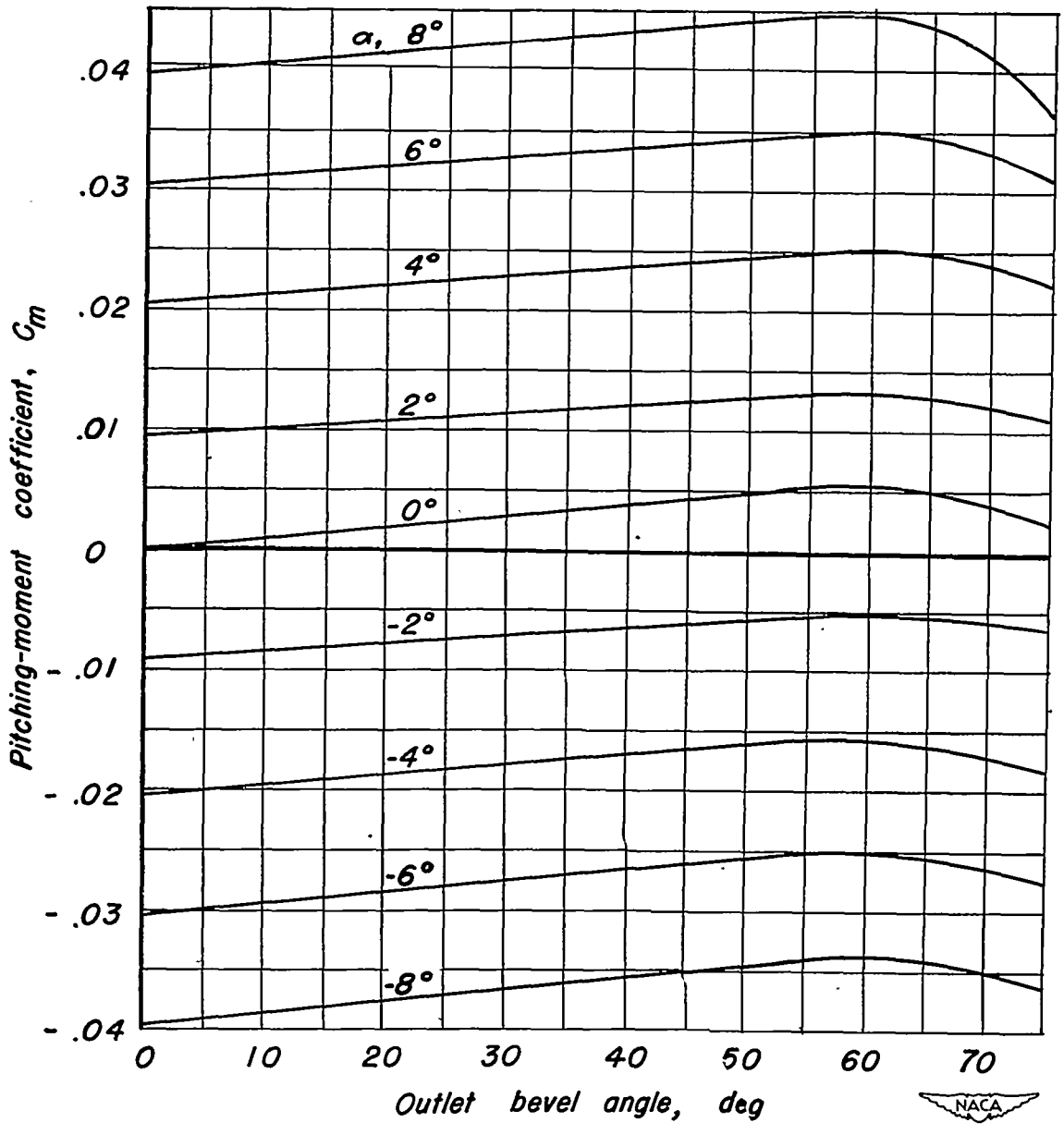

Figure 8.– Variation of pitching–moment coefficient with outlet bevel angle from jet–off tests. V_j/V_0, 0.

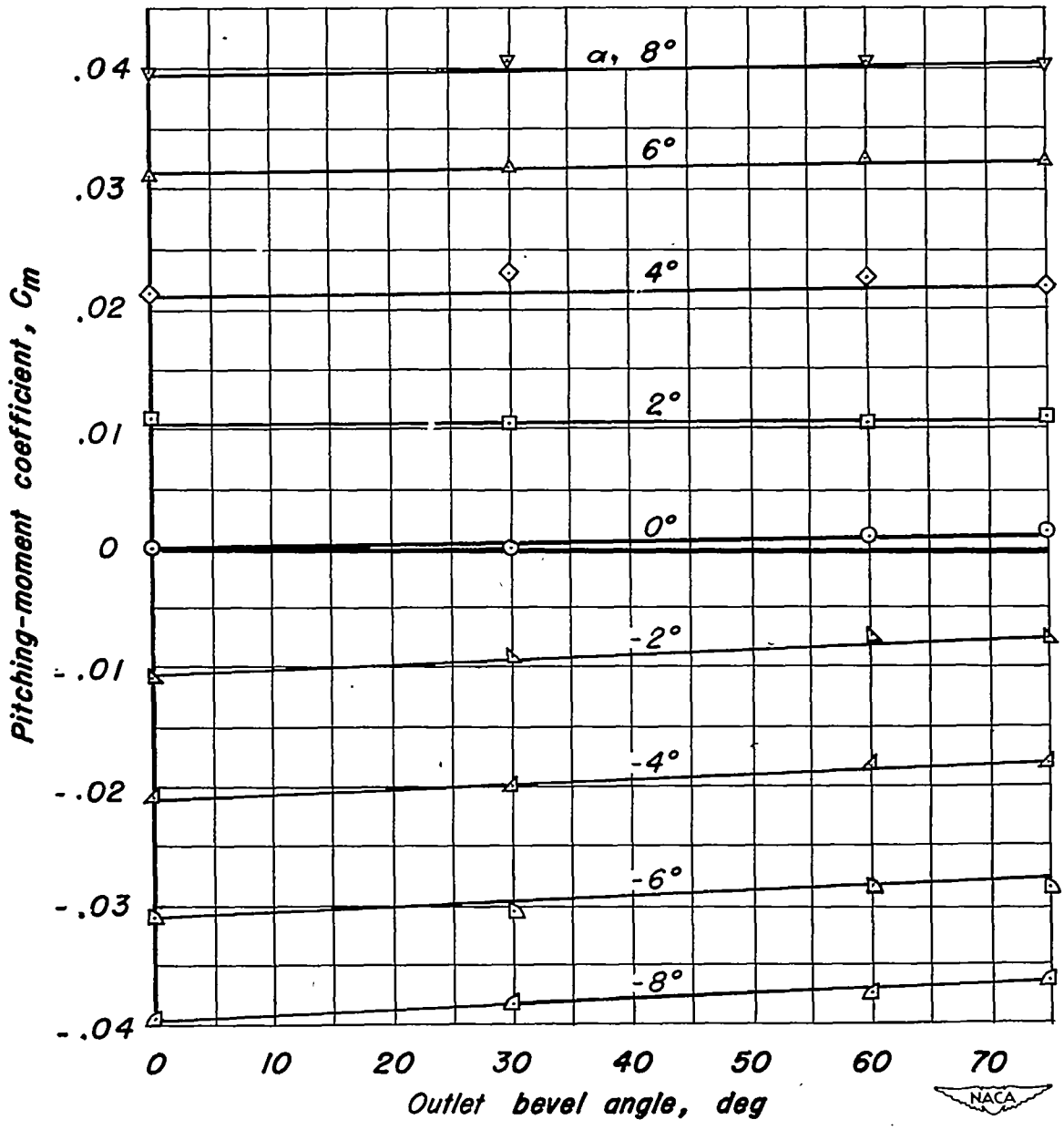

(a) V_j/V_0, 2.0

Figure 9.– Variation of pitching–moment coefficient with outlet bevel angle from jet–on tests.

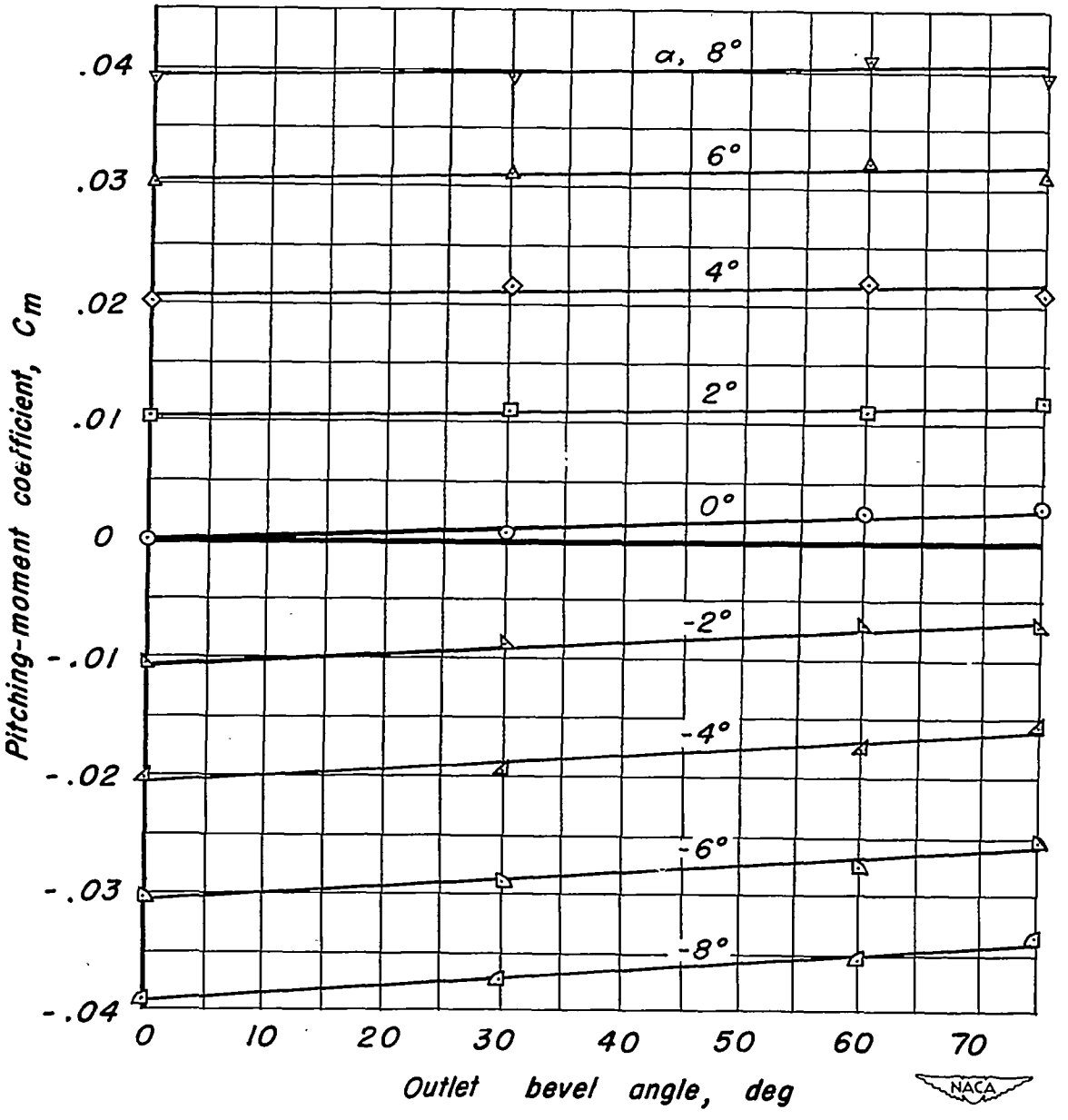

(b) V_j / V_o, 3.0

Figure 9.—Continued.

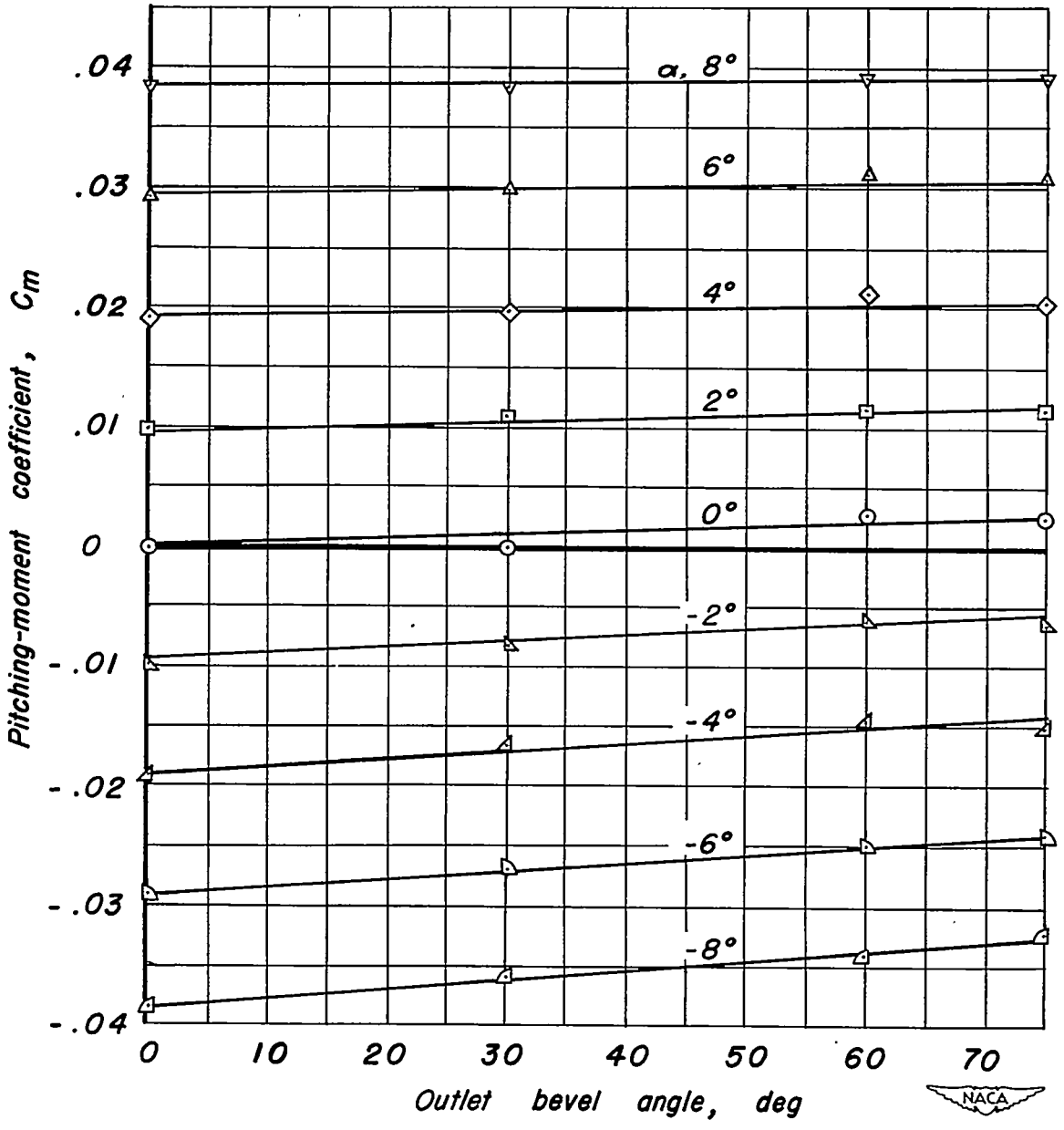

(c) V_j / V_o, 4.0

Figure 9.– Concluded.

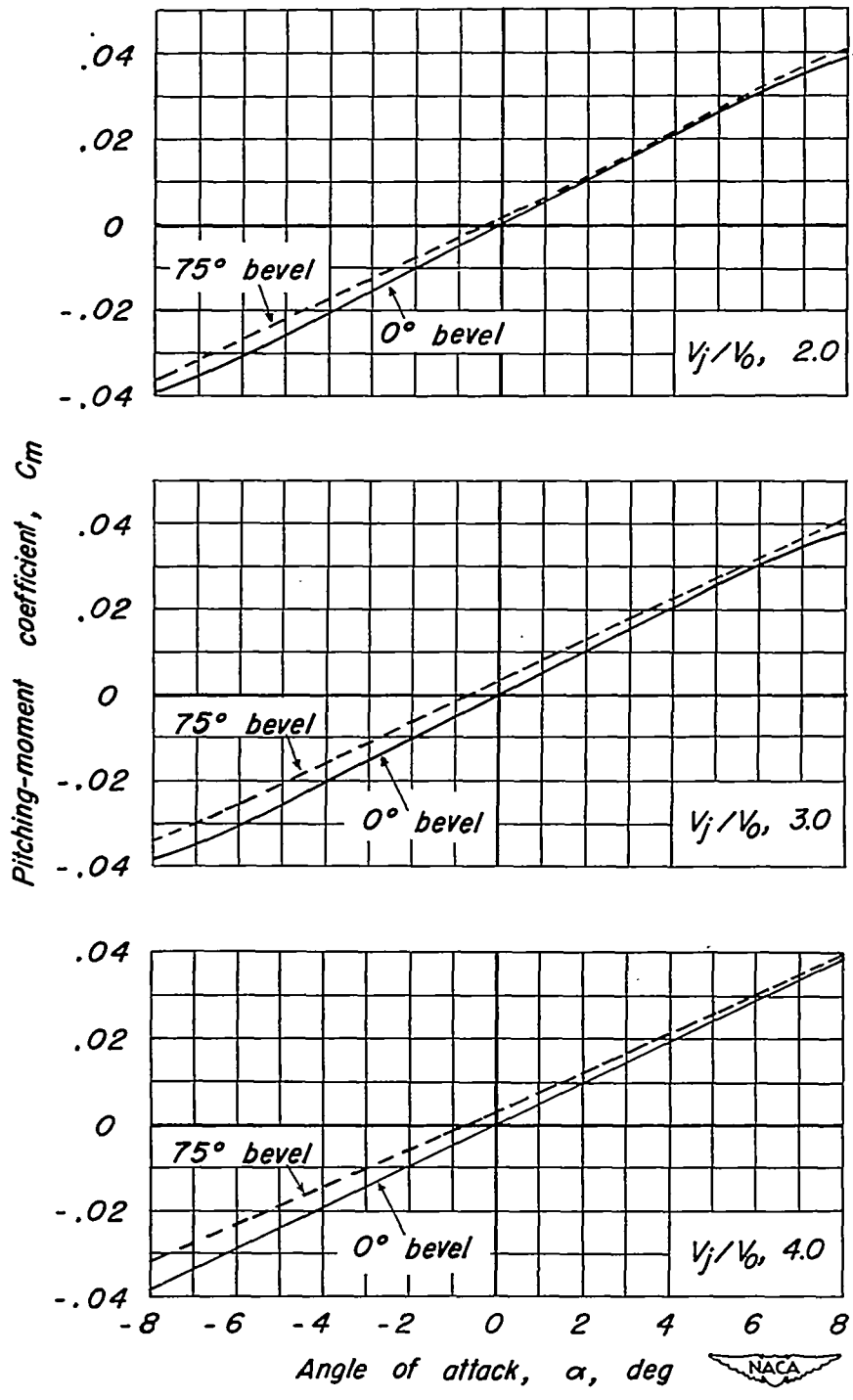

Figure 10.— Variation of pitching-moment coefficient with angle of attack from jet-on tests.

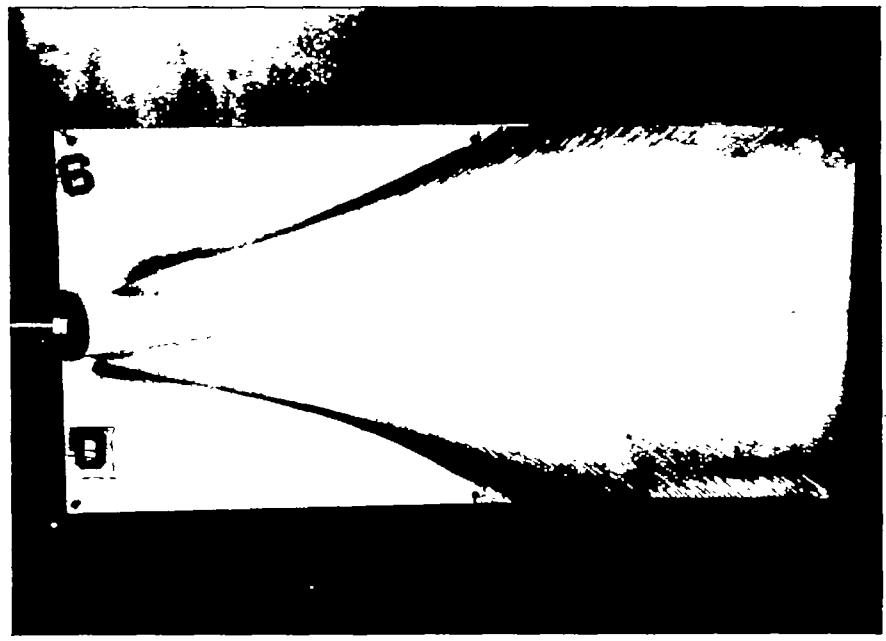

(a) M_j, 0.6

(b) M_j, 0.8

NACA
A-15642

Figure 11.- Flow pictures of jet exhausting into still air for two jet Mach numbers. 0^o-bevelled outlet.

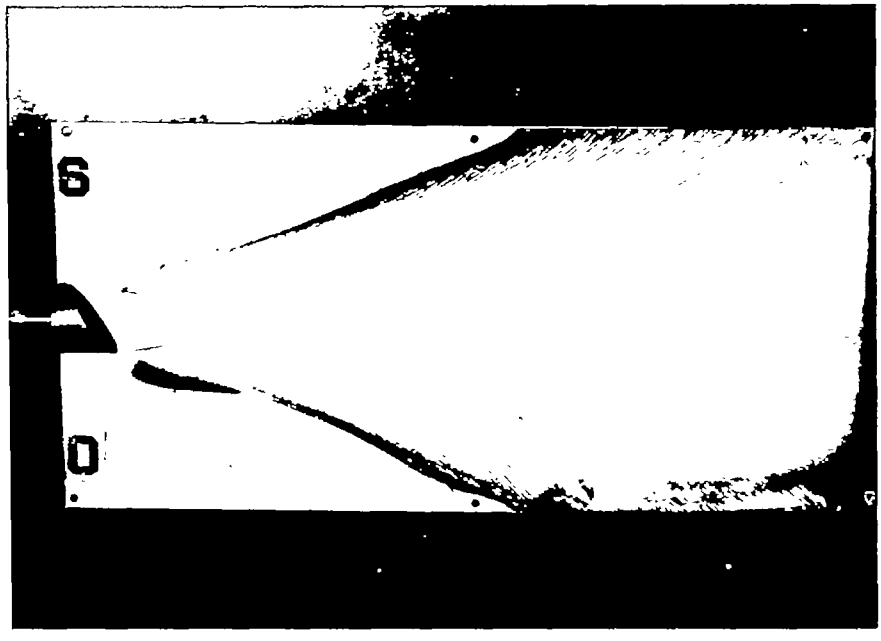

(a) M_j, 0.6

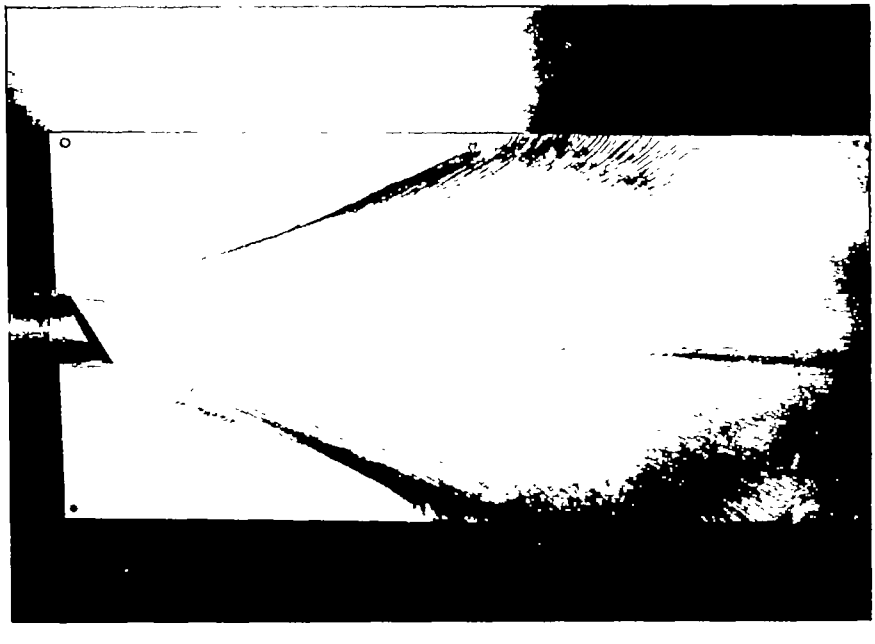

(b) M_j, 0.8

NACA
A-15643

Figure 12.– Flow pictures of jet exhausting into still air for two jet Mach numbers. 30°–bevelled outlet.

(a) M_j, 0.6

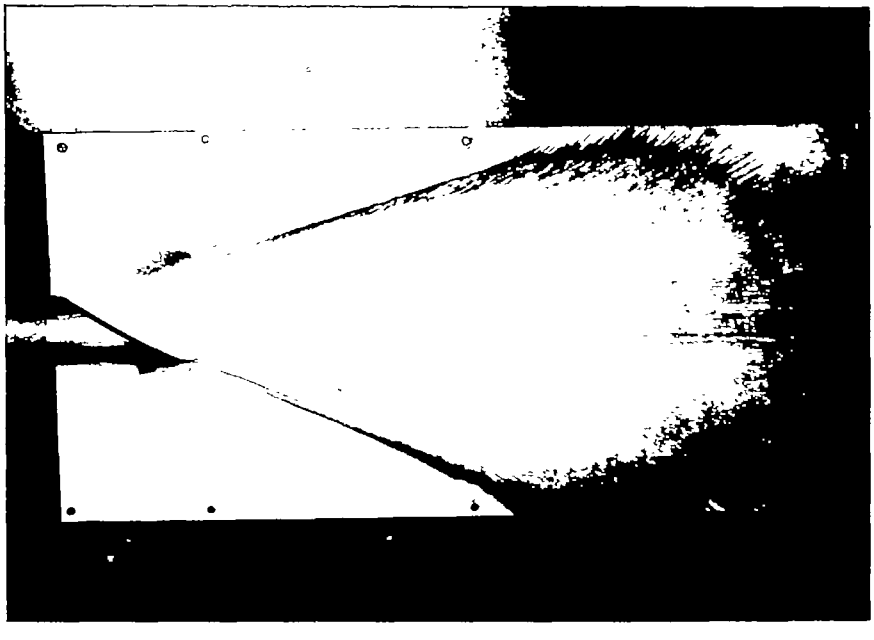

(b) M_j, 0.8

NACA
A-15644

Figure 13.- Flow pictures of jet exhausting into still air for two jet Mach numbers. 60°-bevelled outlet.

(a) M_j, 0.6

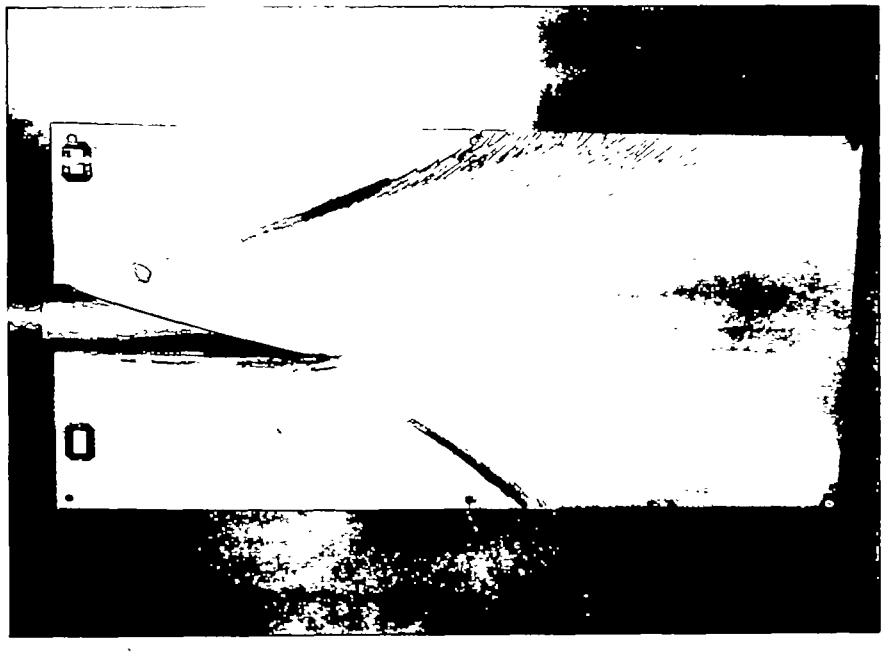

(b) M_j, 0.8

NACA
A-15645

Figure 14.– Flow pictures of jet exhausting into still air for two jet Mach numbers. 75°– bevelled outlet.

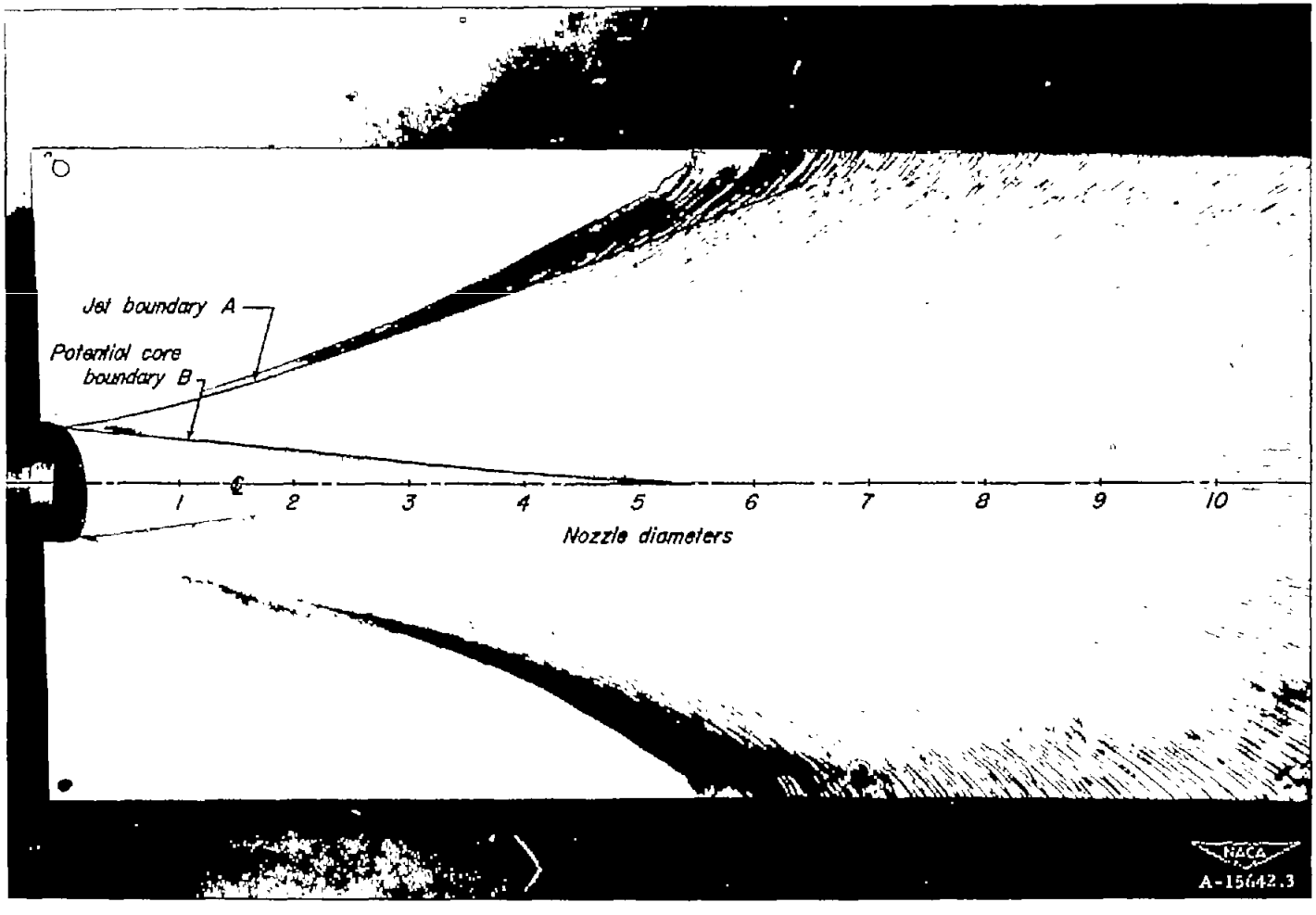

Figure 15.– Flow picture for 0°-bevelled outlet with jet exhausting into still air, showing boundaries of flow regions in the jet. M_j, 0.8.

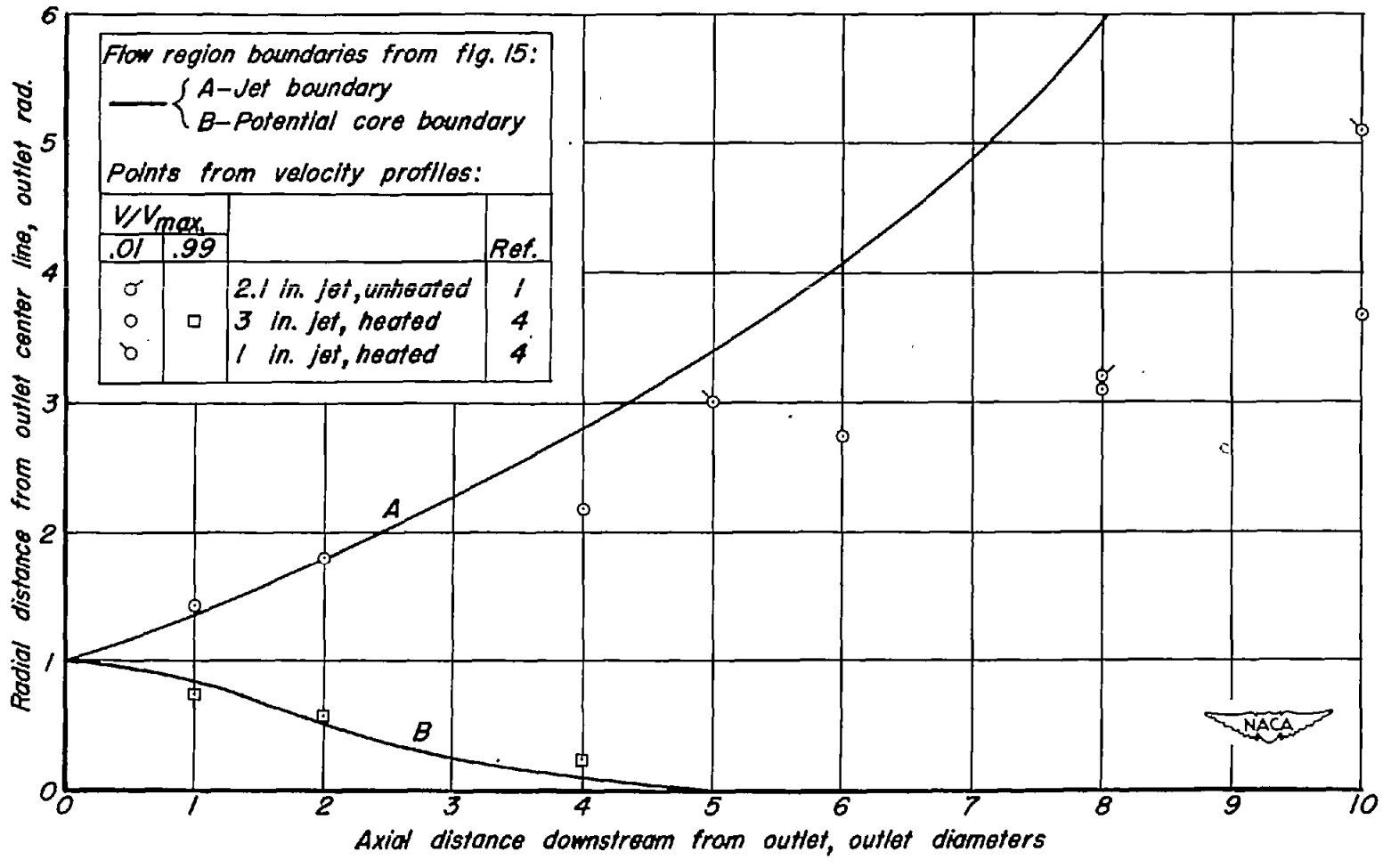

Figure 16.—Dimensionless plot comparing flow regions determined from figure 15 with points determined from velocity profiles measured in other investigations.

NACA-Langley - 6-11-51 - 1000